İSMET KAYA[1)*)], FATİH DOĞAN[2)]

# Synthesis, characterization, and thermal degradation process of poly-4-[(4-hydroxy-2-methylphenyl)iminomethyl]-2,6-dimethylphenol

**Summary** — Schiff base polymer [P-4-HMPIMP] of 4-[(4-hydroxy-2-methylphenyl)iminomethyl]-2,6-dimethylphenol (4-HMPIMP) was synthesized *via* oxidative polycondensation reaction in an alkaline medium with using NaOCl, $H_2O_2$ or air as oxidants. The structures of the synthesized monomer and polymer were confirmed by FT-IR, UV-Vis, NMR and elemental analysis, while their properties were characterized by TG-DTA, size exclusion chromatography (SEC) and solubility tests. The influence of the type of oxidizer on $M_n$, $M_w$ and *PDI* values was also studied. Conductivity measurements of the polymer was done by electrometer using four point probe technique and the electrochemical and optical band gap values of both 4-HMPIMP and P-4-HMPIMP were determined by using cyclic voltammetry and UV-Vis measurements. Conductivity and band gap values indicate that this polymer is a typical semiconductor.

**Key words**: poly-4-[(4-hydroxy-2-methylphenyl)iminomethyl]-2,6-dimethylphenol, synthesis, band gap, conductivity, thermal analysis.

## OTRZYMYWANIE, CHARAKTERYSTYKA I PROCES DEGRADACJI TERMICZNEJ POLI-4-[(4-HYDROKSY-2-METYLOFENYLO)IMINOMETYLO]-2,6-DIMETYLOFENOLU

**Streszczenie** — Wymieniony w tytule polimer (P-4-HMPIMP) typu polizasady Schiffa otrzymywano metodą utleniającej polikondensacji odpowiedniego monomeru (4-HMPIMP) (schemat A) w zasadowym środowisku roztworu KOH, z zastosowaniem jako środków utleniających NaOCl, $H_2O_2$ bądź powietrza. Określono wpływ warunków procesu, rodzaju i stężenia środka utleniającego, temperatury (40—80 °C) oraz czasu trwania (5—20 h) na wydajność P-4-HMPIMP (tabela 1). Budowę monomeru i polimeru scharakteryzowano na podstawie widm FT-IR (rys. 1), $^{1}H$ NMR (rys. 2) oraz $^{13}C$ NMR a także analizy elementarnej. Przedstawiono też wyniki badania metodami cyklicznej woltametrii (rys. 3), UV-Vis (rys. 4), przewodnictwa elektrycznego (rys. 5) i przebiegu krzywych TG-DTG-DTA(rys. 6 i 7). Wartości $M_n$ i $M_w$ oraz polidyspersyjność próbek P-4-HMPIMP otrzymanych wobec różnych środków utleniających uzyskiwano metodą chromatograficzną SEC (tabela 2). Wyniki te posłużyły do szczegółowego scharakteryzowania elektrochemicznych i optycznych (poziomy energetyczne oraz położenia pasm wzbronionych, tabela 3) a także kinetycznych i termodynamicznych parametrów procesu degradacji termicznej wyznaczonych trzema różnymi metodami: Coatsa-Redterna, Mac Callma-Tannera, van Krevelena (tabela 4, rys. 8—10).

**Słowa kluczowe**: poli-4-[(4-hydroksy-2-metylofenylo)iminometylo]-2,6-dimetylofenol, synteza, pasmo wzbronione, przewodnictwo, analiza termiczna.

Polyazomethines (PAMs) containing -HC=N- group in their structures, known as polyimines or Schiff bases polymers, were prepared for the first time from terephthalaldehyde, benzidine and dianisidine in 1923 by Adams and co-workers [1]. This class of polymers has attracted much attention because of their useful properties and wide application fields. Due to the conjugated bonding and active hydroxyl group, in their structure, phenolic polymers substituted with azomethine group possess useful properties such as paramagnetism, semi-conductivity, electrochemical cell and resistance to high energy. They have therefore found applications in the preparation of composites resistant to high temperature, thermostabilizers and graphite materials, epoxy oligomers and block copolymers, adhesives, photoresistors and antistatic materials [2—8]. The addition of halogen, sulfur derivatives or other functional groups to these compounds led to a wider range of useful properties such as enhancing flame-resistance in composite materials of specific detergents [9], removal of poisonous heavy metals in in-

---

[1)] Çanakkale Onsekiz Mart University, Faculty of Sciences and Arts, Polymer Analysis Laboratory 17020, Çanakkale, Turkey.

[2)] Çanakkale Onsekiz Mart University, Faculty of Education, Secondary Science and Mathematics Education 17100, Çanakkale, Turkey.

[*)] To whom all correspondence should be addressed; e-mail: kayaismet@hotmail.com

dustrial wastewaters. The synthesis of polymer-metal complexes is therefore very important in analytic and environmental chemistry.

In recent years, considerable effort has been directed towards the synthesis of conjugated polymers with low optical band gaps ($E_g$), because they exhibit intrinsic electrical conductivity. For this reason, the conductivity and electrochemical properties of some PAMs and their metal complexes was investigated by Kaya *et al.* [10, 11]. For the past two decades, conjugated PAMs have generated considerable interest because of their electronic, optoelectronic, electrochemical and non-linear optical properties [12].

In this paper we have investigated the effects of different parameters such as temperature, time and initial concentrations of oxidants (air, NaOCl, $H_2O_2$) for the preparation of poly-4-[(4-hydroxy-2-methylphenyl)iminomethyl]-2,6-dimethylphenol (P-4-HMPIMP). Both the monomer and polymers were characterized by spectral, thermal and SEC techniques. The electrochemical energy gaps ($E'_g$) of 4-HMPIMP and P-4-HMPIMP were calculated from cyclic voltammogram measurements. The electrical properties of undoped and doped with $I_2$ P-4-HMPIMP were determined by a four-point probe technique at ambient conditions. The kinetic and thermodynamic parameters of thermal degradation of 4-HMPIMP and P-4-HMPIMP were also investigated by MacCallum-Tanner (MC), Coats-Redfern (CR) and van Krevelen (vK) methods.

## EXPERIMENTAL

### Materials

4-hydroxy-3,5-dimethylbenzaldehyde and 4-amino-3-methylphenol were purchased from Alfa Aesar Chemical Co.; tetrahydrofuran (THF), dimethylformamide (DMF), dimethylsulfoxide (DMSO), acetone, ethyl acetate, acetonitrile, dioxane, hexane, heptane, $H_2O_2$ (30 % aqueous solution), KOH, HCl (37 %), $CCl_4$ and $CHCl_3$ were obtained from Merck and used as received. Sodium hypochloride (NaOCl) (30 % aqueous solution) was supplied by Paksoy Chemical Co. (Turkey).

### Preparation of 4-[(4-hydroxy-2-methylphenyl)iminomethyl]-2,6-dimethylphenol

4-HMPIMP was prepared by boiling the mixture of 4-hydroxy-3,5-dimethylbenzaldehyde (1.50 g, 0.01 mol) and 4-amino-3-methylphenol (1.23 g, 0.01 mol) in methanol (25 mL) under reflux for 3 h at 70 °C (see Scheme A). The precipitated 4-[(4-hydroxy-2-methylphenyl)iminomethyl]-2,6-dimethylphenol (4-HMPIMP) was filtered, recrystallized from methanol and dried under vacuum (90 % yield).

Elemental analysis: Calcd. for 4-HMPIMP: C, 75.29; H, 6.67; N, 5.49. Found: C, 75.10; H, 6.51; N, 5.34.

FT-IR ($cm^{-1}$): ν(O-H) 3341 s, ν(C-H Phenyl) 3020 s, ν(C-H aliphatic) 2967 s, ν(C=N) 1622 s, ν(C=C of Ar) 1591, 1492, ν(C-O) 1292 s.

$^1H$ NMR (DMSO): δ ppm, 9.06 (s, 2H, -OH), 8.26 (s, 1H, -CH=N-), 7.50 (s, 2H, Ar-$H_{aa'}$), 6.91 (d, 1H, Ar-$H_b$), 6.72 (s, 1H, Ar-$H_c$), 6.67 (d, 1H, Ar-$H_d$), 2.30 (s, 3H, -$CH_3$), 2.26 (s, 6H, 2-$CH_3$).

$^{13}C$ NMR (DMSO): δ ppm, 155.74 (C1-ipso), 118.54 (C2), 129.26 (C3), 128.52 (C4-ipso), 17.10 (C5), 157.01 (C6), 142.90 (C7-ipso), 133.74 (C8-ipso), 117.32 (C9), 156.55 (C10-ipso), 113.74 (C11), 124.82 (C12), 18.30 (C13).

### Synthesis of poly-4-[(4-hydroxy-2-methylphenyl)iminomethyl]-2,6-dimethylphenol

P-4-HMPIMP was synthesized by the oxidative polycondensation of 4-HMPIMP [13] in aqueous solution (30 %) of NaOCl, $H_2O_2$ (30 %) or in the air atmosphere (see Scheme A).

The 4-HMPIMP (2.55 g, 0.01 mol) dissolved in an aqueous solution of KOH (1 M, 2 mL) was placed in a 50 mL three-necked round-bottom flask fitted with a condenser, thermometer, stirrer and a tap-funnel containing NaOCl. The system was maintained at room temperature and NaOCl (runs 1—13) or $H_2O_2$ (runs 14—24) were added dropwise for about 20 min. The reaction mixtures were stirred at various temperatures and durations (see Table 1 in further text).

Air was passed through an aqueous solution of KOH (1 M, 2 mL) to neutralize the $CO_2$ contained in it before being sent to the reaction to prevent water loss (runs 25—33). The mixture was neutralized after the reaction with 0.03 mol HCl (37 %) at room temperature and the unreacted monomer was separated from the products by washing with ethanol. Mineral salts were separated by filtering the mixture and washing in 25 mL of hot water three times before drying in a vacuum oven at 60 °C.

FT-IR ($cm^{-1}$): ν(O-H) 3219 s, ν(C-H of Ar) 3012 m, ν(C-H aliphatic) 2975 s, ν(C=N) 1603 s, ν(C=C of Ar) 1586, 1499 s, ν(C-O) 1292 s, νC(Ar)-O-C(Ar) and C(Ar)-O-H 1209 m, νC(Ar)-O-C(Ar) 1106 m.

$^1H$ NMR (DMSO): δ ppm, 9.73 (s, 2H, -OH), 7.95 (s, 1H, -CH=N-), 7.48 (s, 2H, Ar-$H_{aa'}$), 7.17 (d, 1H, Ar-$H_b$), 6.95 (s, 1H, terminal-Ar-$H_c$), 6.74 (d, 1H, terminal-Ar-$H_d$), 2.89 (s, 3H, -$CH_3$), 2.73 (s, 3H, -$CH_3$), 2.60 (s, 3H, -$CH_3$).

$^{13}C$ NMR (DMSO): δ ppm, 156.85 (C1-*ipso*), 118.68 (C2), 133.16 (C3), 130.79 (C4-*ipso*), 33.95 (C5), 162.90 (C6), 145.79 (C7-*ipso*), 135.30 (C8-*ipso*), 120.10 (C9), 159.47 (C10-*ipso*), 116.32 (C11), 124.21 (C12), 40.53 (C13), 126.32 and 128.95 (new peaks of C-C and C-O couplings).

### Methods of testing

The infrared spectra were measured by a Perkin Elmer FT-IR Spectrum One using an ATR attachment (4000—550 $cm^{-1}$).

4-HMPIMP and P-4-HMPIMP were characterized also by $^1$H NMR and $^{13}$C NMR (Bruker Avance DPX-400 and 100.6 MHz, respectively) performed at 25 °C, in the presence of deuterated DMSO as solvent and tetramethylsilane as internal standard.

Thermal analysis (TG-DTA) was performed on a Perkin Elmer Diamond Thermal Analysis in the 10—1000 °C temperature range ($N_2$, ramping rate — 10 °C/min).

DSC analysis of P-4-HMPIMP was carried out (30—420 °C, in $N_2$, ramping rate 20 °C/min) on a Perkin Elmer Pyris Saphire DSC.

The number average molecular weight ($M_n$), weight average molecular weight ($M_w$) and polydispersity index (*PDI*) values were determined by Shimadzu Co. size exclusion chromatography (SEC) techniques using an SGX (100 Å and 7 nm diameter loading material) 3.3 mm (internal diameter) × 300 mm column [eluent: DMF/methanol (v/v = 4/1, 0.4 mL/min), polystyrene standards]. A refractive index detector was used to analyze the polymer at 25 °C.

The conductivity of the compounds was measured on a Keithley 2400 electrometer. Pellets were made in a hydraulic press applying 1687.2 kg·cm$^{-2}$ pressure. Iodine doping was carried out by exposing the pellet to iodine vapor at atmospheric pressure and room temperature in a desiccator [7].

The optical band gaps ($E_g$) of 4-HMPIMP and P-4-HMPIMP were calculated from their absorption edges [14]. Their ultraviolet-visible absorption (UV-Vis) spectra were obtained with a Perkin Elmer Lambda 25 at 25 °C in methanol and DMSO, respectively.

The electrochemical properties of the products were determined by CH instruments 660C cyclic voltammetry with 0.1 M tetrabutylammonium hexafluorophosphate ($TBAPF_6$) as supporting electrolyte. The voltammetric measurements were carried out for the monomer and the polymer in acetonitrile and DMSO, respectively. The HOMO and LUMO energy levels were determined from the onset potentials of the *n*-doping ($\phi'_n$) and *p*-doping ($\phi'_p$), respectively, according to the literature [15].

## RESULTS AND DISCUSSION

### FT-IR, NMR, SEC analyses and solubility

The FT-IR spectra of oxidative polycondensation product of 4-[(4-hydroxy-2-methylphenyl)iminomethyl]-2,6-dimethylphenol differ from that of the monomer only by a reduction of the band strength and number of bands -OH and -CH=N group absorption bands were observed at 3341 and 1622 cm$^{-1}$ and at 3219 and 1603 cm$^{-1}$ for the monomer and polymer, respectively (Fig. 1). Moreover C(Ar)-O-C(Ar) and C(Ar)-O-H or C(Ar)-O-C(Ar) bending vibrations were observed in 1209 and 1106 cm$^{-1}$, respectively for P-4-HMPIMP.

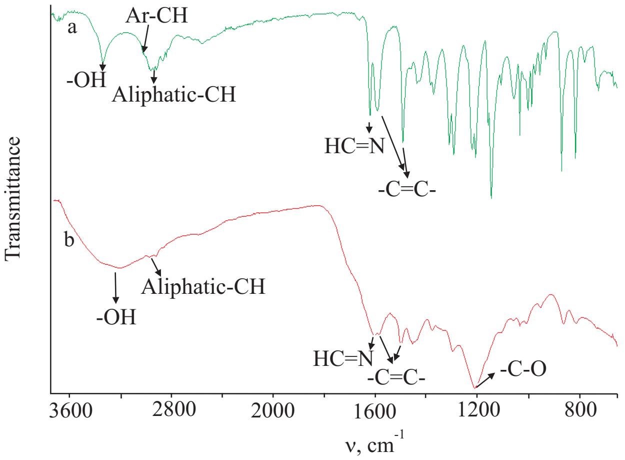

*Fig. 1. FT-IR spectra of 4-HMPIMP (a), P-4-HMPIMP (b)*

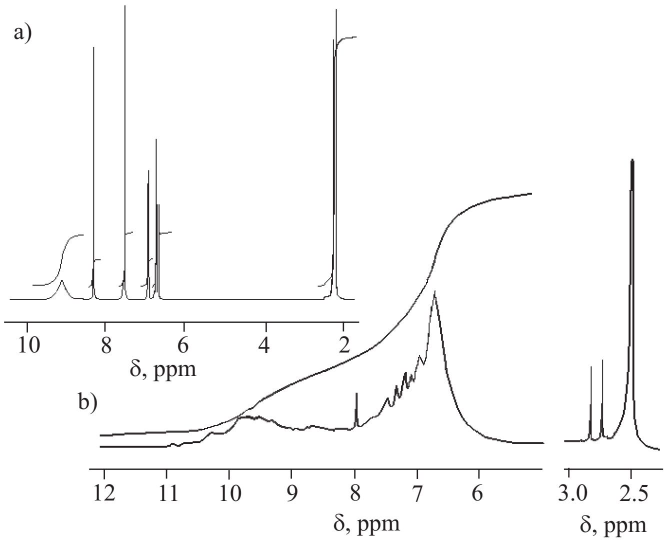

*Fig. 2. $^1$H NMR spectra of 4-HMPIMP (a), P-4-HMPIMP (b)*

The structures of the products were determined also by performing $^1$H NMR and $^{13}$C NMR analysis in DMSO-$d_6$. $^1$H NMR spectra are presented in Fig. 2. So -OH and -CH=N group signals were observed at 9.06 and 8.26 ppm and 9.73 (a) and 7.95 ppm (b) for the monomer and polymer, respectively. Other phenol derivatives were also polymerized as reported in the literature [16]. Cross-linking in polymer structure is expected in the cases where the *ortho* position of the corresponding monomer is unsubstituted. $^1$H NMR and $^{13}$C NMR studies on P-4-HMPIMP indicate that the linkage between any two adjacent phenyl rings is largely at *ortho* position and oxyphenylene. This type of linkage may strain the polymer backbone in such a manner that the phenyl rings are displaced out of plane with respect to the adjacent rings. The peak values of C1, C9, C10 and C11 carbon atoms were observed at 155.74, 117.32, 156.55 and 113.74 ppm for the monomer, and at 156.85, 120.10, 159.47 and 116.32 ppm, for the polymer. New peaks appeared at 126.30 and 128.95 ppm in the $^{13}$C NMR spectrum of polymer. The hydroxyl groups are involved in the formation of free radicals leading to polymer formation and C-O coupling system appeared according to proton integration of peak at the $^{1}$H NMR spectrum of polymer. This confirms that the phenyl rings in the polymer are most probably linked primarily at *ortho* position and oxyphenylene. $^{1}$H NMR and $^{13}$C NMR results showed that the polymerization of 4-HMPIMP was propagated by C-C and C-O coupling from *ortho* position according to -OH group and oxyphenylene, respectively [17]. The coupling selectivity reaction mechanism has been studied by Kaya *et al.* and three possible pathways for C-C and C-O coupling selectivity and Schiff base monomer and dimer interconversion combinations of radical units were proposed [18] (Scheme A).

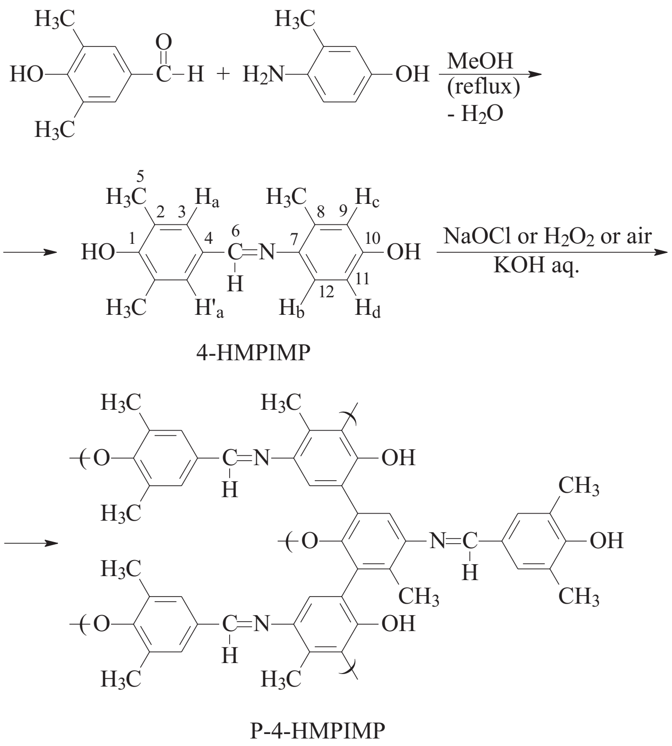

*Scheme A. Synthesis of 4-HMPIMP and P-4-HMPIMP*

4-HMPIMP was in the form of a grey powder completely soluble in organic polar solvents such as methanol, ethanol, acetone, THF, acetonitrile, ethyl acetate, 1-butanol, chloroform, DMF, and DMSO, but insoluble in organic apolar solvents (*e.g.* heptane and hexane). P-4-HMPIMP was in the form of a dark brown powder completely soluble in chloroform, DMF and DMSO, partly soluble in ethanol, methanol, acetone, ethyl acetate and THF, but insoluble in acetonitrile, 1-butanol, heptane and hexane.

## The influence of synthesis parameters on yield and molecular weight of P-4-HMPIMP

The reaction conditions for the oxidative polycondensation of 4-[(4-hydroxy-2-methylphenyl)iminomethyl]-2,6-dimethylphenol using air, $H_2O_2$ or NaOCl as oxidant in an aqueous alkaline medium were investigated and the results presented in Table 1. On contact with these oxidants, brown phenoxy radicals were immediately formed, which precipitated from the reaction mixture. The highest P-4-HMPIMP yields obtained for the oxidants were 86 (run 8), 72 (run 32) and 69 % (run 20) for NaOCl, $O_2$ and $H_2O_2$, respectively. Thus, the most active catalyst was NaOCl. The yields of the polymerization product was also dependent on temperature, reaction time, and the initial concentration of the oxidizer and KOH.

**Table 1. Parameters of the oxidative polycondensation reaction 4-HMPIMP[*)] with NaOCl (runs 1—13), $H_2O_2$ (runs 14—24) or air (runs 25—33) in aqueous KOH**

| Run | $[KOH]_o$ mol $L^{-1}$ | $[NaOCl]_o$ mol·$L^{-1}$ or $[H_2O_2]$, mol·$L^{-1}$ or air, L/h | Temp. °C | Time h | Yield of P-4-HMPIMP % |
|---|---|---|---|---|---|
| 1 | 0.15 | 0.05 | 40 | 5 | 54 |
| 2 | 0.15 | 0.05 | 50 | 5 | 60 |
| 3 | 0.15 | 0.05 | 60 | 5 | 68 |
| 4 | 0.15 | 0.05 | 70 | 5 | 74 |
| 5 | 0.15 | 0.05 | 80 | 5 | 79 |
| 6 | 0.15 | 0.05 | 90 | 5 | 68 |
| 7 | 0.15 | 0.05 | 80 | 10 | 81 |
| 8 | 0.15 | 0.05 | 80 | 15 | 86 |
| 9 | 0.15 | 0.05 | 80 | 20 | 65 |
| 10 | 0.075 | 0.05 | 80 | 5 | 53 |
| 11 | 0.20 | 0.05 | 80 | 5 | 61 |
| 12 | 0.15 | 0.1 | 80 | 5 | 68 |
| 13 | 0.15 | 0.15 | 80 | 5 | 56 |
| 14 | 0.15 | 0.05 | 40 | 5 | 29 |
| 15 | 0.15 | 0.05 | 50 | 5 | 43 |
| 16 | 0.15 | 0.05 | 60 | 5 | 60 |
| 17 | 0.15 | 0.05 | 70 | 5 | 65 |
| 18 | 0.15 | 0.05 | 80 | 5 | 59 |
| 19 | 0.15 | 0.05 | 90 | 5 | 50 |
| 20 | 0.15 | 0.05 | 70 | 10 | 69 |
| 21 | 0.15 | 0.05 | 70 | 15 | 56 |
| 22 | 0.15 | 0.05 | 70 | 20 | 53 |
| 23 | 0.15 | 0.1 | 70 | 10 | 62 |
| 24 | 0.15 | 0.15 | 70 | 10 | 55 |
| 25 | 0.15 | 8.5 | 40 | 5 | 27 |
| 26 | 0.15 | 8.5 | 50 | 5 | 43 |
| 27 | 0.15 | 8.5 | 60 | 5 | 50 |
| 28 | 0.15 | 8,5 | 70 | 5 | 54 |
| 29 | 0.15 | 8.5 | 80 | 5 | 61 |
| 30 | 0.15 | 8.5 | 90 | 5 | 51 |
| 31 | 0.15 | 8.5 | 80 | 10 | 65 |
| 32 | 0.15 | 8.5 | 80 | 15 | 72 |
| 33 | 0.15 | 8.5 | 80 | 20 | 61 |

[*)] The initial concentration of 4-HMPIMP = 0.15 mol $L^{-1}$.

**Table 2. Influence of the type of oxidizing agent on the number average molecular weight ($M_n$), weight average molecular weight ($M_w$), polydispersity index (*PDI*) and the weight distribution of fractions I and II of P-4-HMPIMP**

| Oxidizing agent | Molecular weight distribution parameters | | | | | | | | | | |
|---|---|---|---|---|---|---|---|---|---|---|---|
| | Total | | | Fraction I | | | | Fraction II | | | |
| | $M_n$ | $M_w$ | *PDI* | $M_n$ | $M_w$ | *PDI* | % | $M_n$ | $M_w$ | *PDI* | % |
| Air | 19 100 | 21 600 | 1.131 | 13 400 | 15 200 | 1.134 | 60 | 75 500 | 85 100 | 1.127 | 40 |
| NaOCl | 23 200 | 26 600 | 1.147 | 12 800 | 15 900 | 1.242 | 55 | 87 500 | 98 700 | 1.128 | 45 |
| | 12 100 | 14 600 | 1.207 | 11 350 | 14 500 | 1.278 | 70 | 54 500 | 63 250 | 1.161 | 30 |

The P-4-HMPIMP $M_n$, $M_n$ and *PDI* values, and also the weight distribution of lower and higher molecular weight fractions are presented in Table 2. The values were calculated on the basis of SEC measurements using the polystyrene standard calibration curve. An obvious influence of the type of oxidant on the results can be observed.

## Electrochemical properties of 4-HMPIMP and P-4-HMPIMP

The voltammograms of 4-HMPIMP and P-4-HMPIMP were carried out with acetonitrile and DMSO, respectively. The HOMO and LUMO levels and electrochemical energy gaps ($E'_g$) were determined from the onset values of oxidation and reduction processes (Fig. 3). The HOMO, LUMO energy levels ($\lambda_{max}$), and optical ($E_g$) electrochemical ($E'_g$) and band gap values of are given in Table 3. So, energy levels and electrochemical band gaps ($E'_g$) of 4-HMPIMP and P-4-HMPIMP were found to be in the range of -5.71— -5.43; -2.65— -2.61; 3.06—2.82; while the electrochemical band gap ($E'_g$) values of monomer and polymer were measured to be 2.87 and 2.48 eV, respectively [19]. The optical band gap ($E_g$) values of 4-HMPIMP and P-4-HMPIMP determined on the basis of the absorption spectra presented in Fig. 4 were found to be 3.15 and 2.76 eV, respectively.

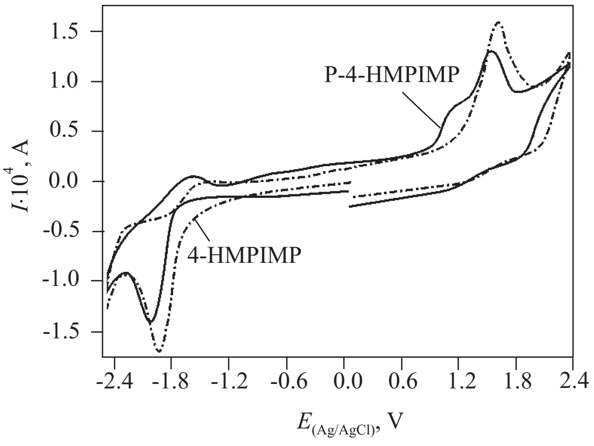

*Fig. 3. Cyclic voltammograms of 4-HMPIMP (1) and P-4-HMPIMP (2)*

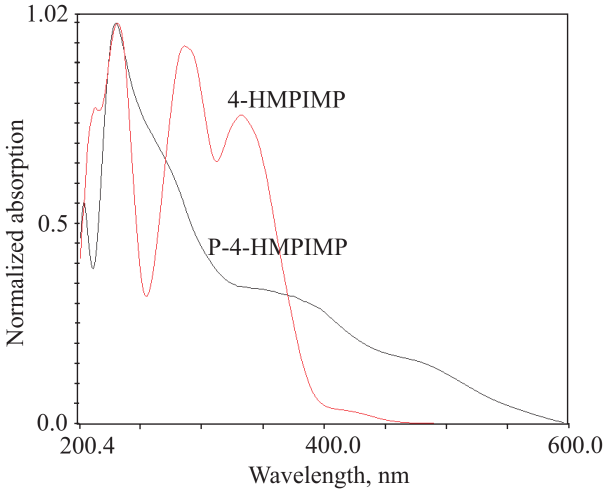

*Fig. 4. Absorption spectra of 4-HMPIMP and P-4-HMPIMP*

**Table 3. Electrochemical and optical parameters of the synthesized compounds[*)]**

| Compound | $\lambda_{max}$, nm | HOMO eV | LUMO eV | $E_g$, eV | $E'_g$, eV |
|---|---|---|---|---|---|
| 4-HMPIMP | 230, 286, 336 | -5.71 | -2.65 | 3.15 | 3.06 |
| P-4-HMPIMP | 232, 482, 375 | -5.43 | -2.61 | 2.76 | 2.82 |

[*)] $\lambda_{max}$ — maximum wavelength, HOMO — the highest occupied molecular orbital, LUMO — the lowest unoccupied molecular orbital, $E_g$ — optical band gap, $E'_g$ — electrochemical band gap.

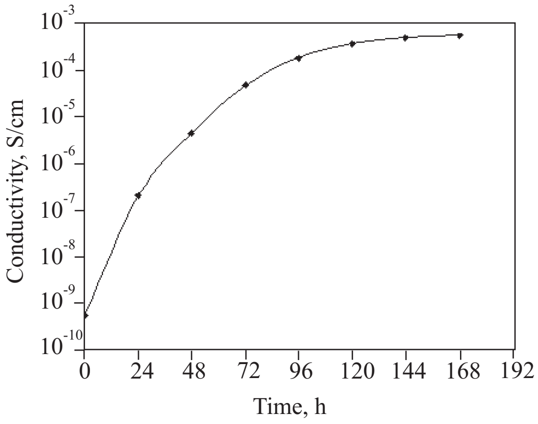

*Fig. 5. Electrical conductivities of $I_2$-doped P-4-HMPIMP versus doping time at 25 °C*

The conductivity of P-4-HMPIMP was found to begin between $10^{-10}$—$10^{-9}$ S $cm^{-1}$; which increased after doping with iodine. Fig. 5 shows the influence of doping duration at 25 °C on conductivity of doped P-4-HMPIMP. The conductivity initially rose sharply with doping duration, but later levelled off at longer periods. This should indicate a continuous formation of a charge transfer complex between the polymer and iodine. The results also indicate the reaction rate on doping. In order to achieve maximum conductivity, a longer doping duration is required. The conductivity/doping time curve varies also with doping conditions. In order to eliminate the influence of doping conditions, the conductivity of the polymer was determined in relation to the doping extent. The maximal (or saturated) conductivity values of P-4-HMPIMP were found to be $7.95 \cdot 10^{-4}$ S $cm^{-1}$.

Diaz *et al.* proposed conductivity mechanisms for Schiff base polymers doped with iodine [7]. Nitrogen is a very electronegative element which is capable of coordinating an iodine molecule. Nitrogen atom coordination of Schiff base polymers and pyridine/iodine solutions has been presented in the literature [20—22].

## Thermal degradation

### Results

TG-DTG-DTA analysis was applied to determine thermal degradation of the studied monomer and polymer and their results presented in Fig. 6 and 7. Degradation of 4-HMPIMP was found to commence at 250 °C while P-4-HMPIMP started to degrade at 254 °C. A weight loss of 74.69 % at 1000 °C was recorded for 4-HMPIMP and for P-4-HMPIMP the value was 25.92 %. A large amount (74.08 %) of carbine residue was formed on the polymer at 1000 °C. DTG analysis showed $T_{max}$ values of 292 and 381 °C for 4-HMPIMP and P-4-HMPIMP, respectively. Exothermic and endothermic peaks were observed at 335 and 204 °C for 4-HMPIMP. TG analysis results indicate that P-4-HMPIMP is more stable thermally and resistant to thermal decomposition than the monomer due to the presence of long conjugated band systems.

The glass transition temperatures ($T_g$) and changes in specific heat during glass transition ($\Delta Cp$) were found to be 179 °C and 0.078 J/g °C, respectively for P-4-HMPIMP.

### Kinetic and thermodynamic parameters

Non-isothermal methods have been extensively used for the study of the kinetics and mechanism of condensed phase reactions [23]. In general, most methods of kinetic analysis of thermoanalytical data begin with the well-known Arrhenius' equation

$$k = A \exp(-E_a / RT) \tag{1}$$

and a rate expression

$$\mathrm{d}\alpha/\mathrm{d}t = kf(\alpha) \tag{2}$$

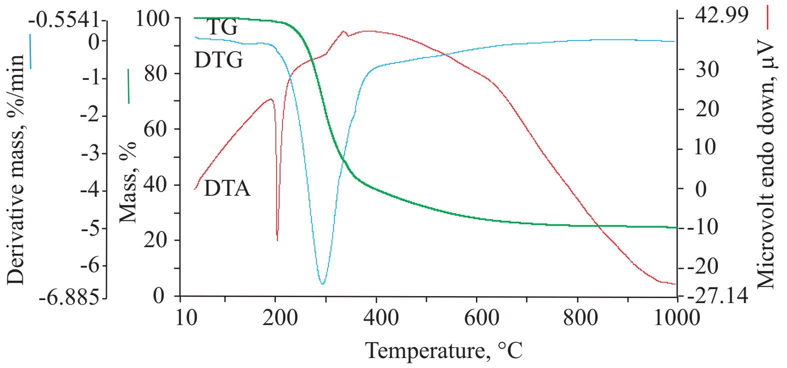

*Fig. 6. TG-DTG-DTA curves of 4-HMPIMP*

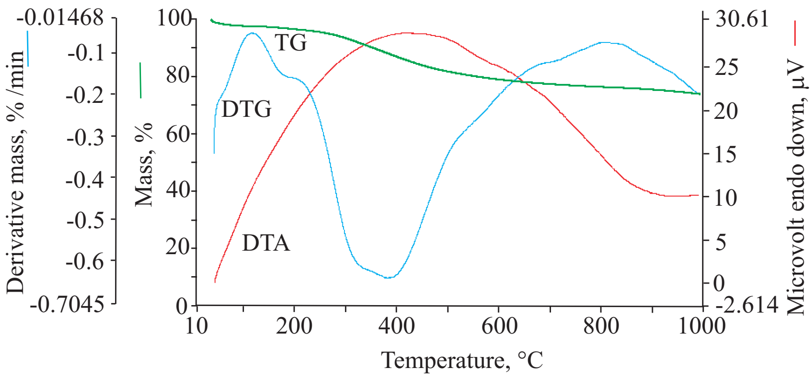

*Fig. 7. TG-DTG-DTA curves of P-4-HMPIMP*

The expression f(α) in equation (2) is the so-called kinetic function that depends on the reaction mechanism, and α is the fractional conversion (from 0 to 1) of the solid reactant.

In a condition where $f(\alpha) = (1 - \alpha)^n$ and a steady temperature rise, $dT/dt = \beta$ (β is the heating rate in °C/min) and then the integration of equation (2) leads to

$$g(\alpha)=\int_0^{\alpha}\left[\frac{1}{(1-\alpha)^n}\right]d\alpha=\frac{A}{\beta}\int_{T_0}^{T}\exp\left(\frac{-E_a}{RT}\right)dT \tag{3}$$

where: *g(α) — rate of degradation, $E_a$ — apparent energy of thermal degradation, n — reaction order.*

For n = 1:

$$\int_0^{\alpha}\left[\frac{1}{(1-\alpha)^n}\right]d\alpha=-\ln(1-\alpha) \tag{4}$$

and for *n* values other than zero or unity:

$$\int_0^{\alpha}\left[\frac{1}{(1-\alpha)^n}\right]d\alpha=-\frac{1-(1-\alpha)^{1-n}}{1-n} \tag{5}$$

Several following techniques have been developed for solving the integral of equation (3).

*The Coats—Redfern (CR) method [24]*

The following equation can be obtained applying an asymptotic approximation for resolution of equation (3):

$$\ln\left[\frac{g(\alpha)}{T^2}\right]=\ln\left[\frac{AR}{\beta E_a}\left(1-\frac{2RT}{E_a}\right)\right]-\left(\frac{E_a}{RT}\right) \tag{6}$$

The authors supposed that $\ln[1 - (2RT/E_a)] \to 0$ for Doyle approximation [25], thereby obtaining:

$$\ln g(\alpha)\cong\ln\left[\frac{AR}{\beta E_a}\right]-\frac{E_a}{RT} \tag{7}$$

in the natural logarithmic form.

The apparent activation energy degradation for each thermal decomposition mechanism can be obtained from the slope of the plot of ln $[g(\alpha)/T^2]$ *versus* 1000/*T*.

*MacCallum—Tanner (MCT) method [26]*

The MacCallum—Tanner method provides an approximation integrated from the rate of degradation as a function of temperature. This can be expressed as:

$$\log g(\alpha)=\log\frac{AE_a}{\beta R}-0.4828E^{0.4351}-\left(\frac{0.440+0.217E_a}{10^{-3}T}\right) \tag{8}$$

The value of $E_a$ can be derived from the plot of log *g*(α) *versus* 1/*T* and the value of *A* — from the intersection of the Y axis.

*van Krevelen (vK) method [27]*

The integration method used by van Krevelen is for $n \neq 1$ expressed by:

$$\ln g(\alpha)=\ln\left[\frac{A(0.368/T_m)^x}{\beta(x+1)}\right]+(x+1)\ln T \tag{9}$$

where: *$x = E_a/RT_m$, and $T_m$ — the temperature at the maximum rate of weight loss.*

$E_a$ can be obtained from the slope of a plot of ln *g*(α) *versus* ln*T*.

In the equations (1)—(9), *g*(α), β, $T_m$, $E_a$, *A*, *R*, *k* represent the integral functions of conversion, heating rate, DTG peak temperature, activation energy ($kJ\cdot mol^{-1}$), pre-exponential factor ($min^{-1}$), gas constant (8.314 $J\cdot mol^{-1}\cdot K^{-1}$) and specific rate constant, respectively. The kinetic parameters were calculated from the linear plots of the left-hand side of kinetic equations (6) and (7) against 1/*T*. For equation (8) the left-hand side is plotted against ln*T*. The $E_a$ and *A* values were calculated from the slope and intercept of the straight lines.

For the investigated methods, the determination of the pre-exponential factor and the reaction order is possible from of *g*(α) in equation (3) where n ≠ 1:

$$g(\alpha)=\frac{1-(1-\alpha)^{1-n}}{1-n} \tag{10}$$

The kinetic data (*n*, $E_a$, ln*A*) obtained by different methods correspond with each other.

The change in values of enthalpy (Δ*H**), entropy (Δ*S**) and the Gibbs free energy (Δ*G**) for the monomer and polymer were calculated using the following relations [26]:

$$\Delta S^*=2.303\log\left(\frac{Ah}{kT}\right)R \tag{11}$$

$$\Delta H^*=E_a-RT \tag{12}$$

$$\Delta G^*=\Delta H-T\Delta S^* \tag{13}$$

where: *h — the Planck constant.*

TGA experiments were performed to determine thermal behavior of monomer and polymer and to evaluate the degradation processes and kinetic parameters. The CR, MCT and vK methods presented above were used for kinetic analysis. The methods were applied using a single heating rate (10 °C $min^{-1}$). The reaction order (*n*), activation energy ($E_a$), pre-exponential factor (*A*), as well as entropies (Δ*S**), enthalpy (Δ*H**) and free energy (Δ*G**) changes were calculated from the TGA curves of the monomer and the polymer and presented in Table 4.

The thermal degradation linearization curves of the samples have been elucidated by the methods mentioned

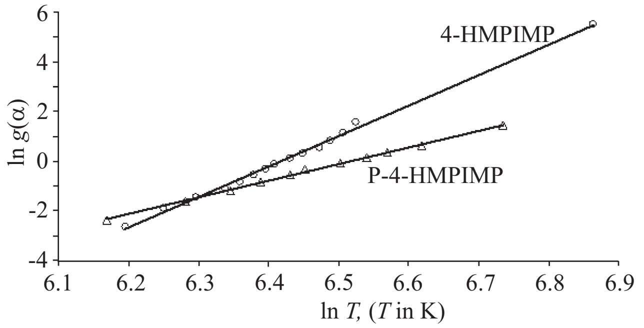

*Fig. 8. vK plots of 4-HMPIMP and P-4-HMPIMP*

**T a b l e 4. Calculated by the different methods the thermodynamic and kinetic parameters of the thermal degradation processes of 4-HMPIMP and P-4-HMPIMP[*)]**

| Compounds | Methods | $n$ | $E_a$, kJ · mol$^{-1}$ | ln$A$ ($A$ in s$^{-1}$) | $\Delta S^*$, kJ · mol$^{-1}$ | $\Delta H^*$, kJ · mol$^{-1}$ | $\Delta G^*$, kJ · mol$^{-1}$ | $r$ |
|---|---|---|---|---|---|---|---|---|
| 4-HMPIMP | vK | 0.3 | 53.28 | 16.80 | -111.78 | 47.82 | 121.15 | 0.99833 |
| | MCT | 0.5 | 55.45 | 14.83 | -128.14 | 49.99 | 134.05 | 0.99736 |
| | CR | 0.5 | 54.51 | 13.12 | -142.0 | 49.47 | 135.57 | 0.98121 |
| P-4-HMPIMP | MCT | 0.3 | 32.91 | 10.47 | -163.21 | 28.20 | 120.58 | 0.99872 |
| | vK | 0.3 | 31.21 | 5.908 | -201.15 | 26.50 | 140.35 | 0.99909 |
| | CR | 0.4 | 33.35 | 9.97 | -168.19 | 28.29 | 130.22 | 0.99012 |

[*)] The meanings of symbols — see text.

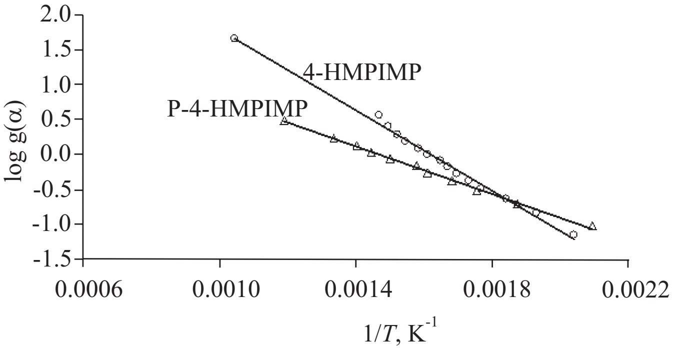

*Fig. 9. MCT plots of 4-HMPIMP and P-4-HMPIMP*

above. The results in Table 4 indicate that the correlation coefficient ($r$) of linearization of these curves is approximately 1.00 and the thermal degradation reaction order is about zero. The results obtained from the different methods are in good agreement so they can be referred to as comparable.

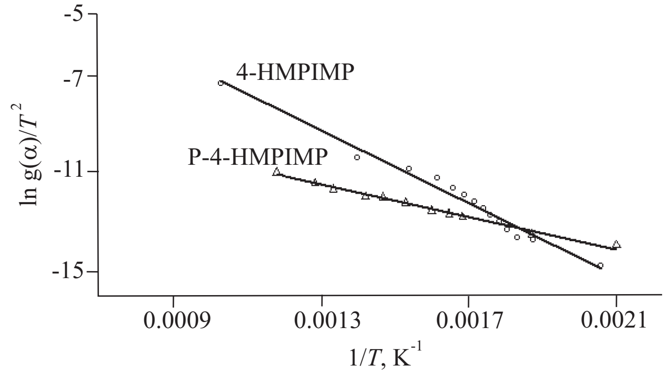

*Fig. 10. CR plots of 4-HMPIMP and P-4-HMPIMP*

The Arrhenius plots for the TG-DTA thermal degradation measurements as determined by the CR, MCT and vK methods are presented in Figs. 8—10.

The kinetic parameters of these processes were calculated by non-isothermal data used in the cases of thermal and thermo-oxidative degradation of polymers and polymeric materials [28, 29].

## CONCLUSION

Poly-4-[(4-hydroxy-2-methylphenyl)iminomethyl]-2, 6-dimethylphenol was synthesized in the oxidative polycondensation of the appropriate monomer. NaOCl, $H_2O_2$ or air in an aqueous alkaline medium were used as oxidizer. The maximal of P-4-HMPIMP yields obtained were 86, 69 and 72 % for NaOCl, $H_2O_2$ and air, respectively. The highest activity was observed with NaOCl as oxidant. $^1$H NMR, $^{13}$C NMR and FT-IR spectral analysis results have confirmed the bondage of *ortho* carbons and oxyphenylene of the phenol ring to obtain the polymer from the oxidative polycondensation of 4-HMPIMP. The optical band gap $E_a$ of the monomer was higher than that of polymer. For both products the HOMO values were higher than the LUMO. The electrochemical band gap $E'_g$ was lower than $E_g$ in the case of monomer; for polymer the situation was inverted.

TGA-DTG-DTA analysis conform a high resistance of the polymer to thermal degradation. TGA experiments can be used to determine the thermal behavior and to evaluate the degradation processes of the studied materials. The thermodynamic of the thermal degradation processes were calculated by the vK, MCT and CR methods.

## REFERENCES

1. Adams R., Bullock R. E., Wilson W. C.: *J. Am. Chem. Soc.* 1923, **45**, 521.
2. Suh S. C., Shim S. C.: *Synth. Met.* 2000, **114** (1), 91.
3. Mamedov B. A., Vidadi Y. A., Alieva D. N., Ragimov A. V.: *Polym. Int.* 1997, **43** (2), 126.
4. Ragimov A. V., Mamedov B. A., Gasanova S. G.: *Polym. Int.* 1997, **43** (3), 343.
5. Baughman R. H., Bredas J. L., Chance R. R., Elsenbaumer R. L., Shacklette L. W.: *Chem. Rev.* 1982, **82**, 209.
6. Kaya İ., Kızılkaya B., Özdemir E.: *Polym. Plast. Technol. Eng.* 2005, **44** (7), 1307.
7. Diaz F. R., Moreno J., Tagle L. H., East G. A., Radic D.: *Synth. Met.* 1999, **100** (2), 187.
8. Aly K. I., Khalaf A. A.: *J. Appl. Polym. Sci.* 2000, **77** (6), 1218.
9. Ehlers F. G., Fisch K. R., Powell W. R.: *J. Polym. Sci. A-1* 1969, **7**, 2931.

10. Kaya İ., Aydın A.: *Polym. Adv. Techn.* 2010, (www.interscience.wiley.com) DOI: 10.1002/pat.1601.
11. Kaya İ., Yıldırım M.: *J. Appl. Polym. Sci.* 2008, **110** (1), 539.
12. Iwan A., Sek D.: *Progress Polym. Sci.* 2008, **33** (3), 289.
13. Kaya İ., Demir H. Ö., Vilayetoğlu A. R.: *Synth. Met.* 2002, **126** (2, 3), 183.
14. Colladet K., Nicolas M., Goris L., Lutsen L., Vanderzande D.: *Thin Solid Films* 2004, **451—452**, 7.
15. Li Y., Cao Y., Jun G., Wang D., Yu G., Heeger A. J.: *Synth. Met.* 1999, **99**, 243.
16. Ayyagari M. S., Marx K. A., Tripathy S. K., Akkara J. A., Kaplan D. L.: *Macromolecules* 1995, **28**, 5192.
17. Kaya İ., Bilici A.: *Synth. Met.* 2006, **156** (9—10), 736.
18. Kaya İ., Bilici A.: *J. Appl. Polym. Sci.* 2007, **104** (5), 3417.
19. Kaya İ., Aydın A.: „*Polym. Adv. Techn*." 2010, **21** (5), 337.
20. Sakai H., Matsuyama T., Maeda Y., Yamaoka H. J.: *J. Chem. Phys.* 1981, **75** (10), 5155.
21. Tassaing T., Besnard M.: *J. Phys. Chem. A* 1997, **101** (8), 2803.
22. Satoh N., Nakashima T., Yamamoto K.: *J. Am. Chem. Soc.* 2005, **127**, 13 030.
23. Keattch C. J., Dollimore D.: „An Introduction Thermogravimetry", London 1975, p. 144.
24. Coats A. W., Redfern J. P.: *Nature* 1964, **201**, 68.
25. Doyle C. D.: *J. Appl. Polym. Sci.* 1961, **5**, 285.
26. MacCallum J. R., Tanner J.: *Eur. Polym. J.* 1970, **6**, 1033.
27. van Krevelen D. W., van Heerden C., Huntjons F. J.: *Fuel* 1951, **30**, 253.
28. Al-Wallan A. A.: *Synth. React. Inorg. Met.-Org. Chem.* 2002, **32**, 489.
29. Budrugeac P.: *Polym. Degrad. Stab.* 2005, **89**, 265.

*Received 17 IV 2009.*